Delayed luminescence of biological systems arising from correlated many-soliton states

Larissa Brizhik*
Bogolyubov Institute for Theoretical Physics, 03143 Kyiv, Ukraine

Agata Scordino,† Antonio Triglia, and Francesco Musumeci
Dipartimento di Metodologie Fisiche e Chimiche per l'Ingegneria, Unità INFM, Università di Catania, viale A. Doria 6, I-95125 Catania, Italy

(Received 5 March 2001; published 14 August 2001)

The kinetics of the delayed luminescence arising from correlated coherent many-soliton states in low-dimensional macromolecular systems, is calculated and shown to be different from the one arising from independent soliton states. The correlation between coherent electron states is essential at relatively high levels of excitation in the presence of very long macromolecules in a system. These conditions can be fulfilled in such biological systems, like algae *Acetabularia Acetabulum.* The cytoskeleton of this unicellular alga contains macromolecular structures (actin filaments, microtubules, etc.) of the length of several hundreds angstroms and more, in which many-soliton coherent states can exist. Indeed, the correlated coherent model is shown to give better fit of the experimental data for this type of algae in a wide range of intensities of the stimulating light, as compared with the model of noncorrelated solitons. The nonlinearity of the dependence of delayed luminescence intensity on the level of excitation increases with the increase of correlation between solitons.

DOI: 10.1103/PhysRevE.64.031902 PACS number(s): 87.15.Mi, 05.45.Yv, 71.35.−y

I. INTRODUCTION

The phenomenon of the delayed luminescence (DL), which consists of photoinduced light emission a long time (seconds and more) after illumination, has been proved to exist not only in solid state systems, but in biological systems as well [1]. It has been actively studied during the last 2 decades and a lot of experimental data have been accumulated. Concerning bio-systems, these studies reveal a number of characteristic properties of this phenomenon, which are sensitive to the chemical, physical, and physiological state of the system and can give the global information about the state of the organism [2–12]. Because of strong correlation between the properties of the DL emission and the biological state of systems, DL is regarded as a powerful tool for medical investigations, food, and water quality control, etc. Among the common characteristics of DL in bio-systems the most essential are the following [11]:

(a) DL kinetics in a wide time interval satisfies the phenomenological Becquerel law, given by the hyperbolic time dependence:

$$I(t)=(a+bt)^{-\alpha}, \tag{1}$$

which becomes linear in a log-log scale;

(b) The various components of the emission spectrum have the same time trends, i.e., the same value of the hyperbolic parameter α in Eq. (1);

(c) The initial intensity of DL, $I(t=0)$, depends on the intensity of the stimulating light in a nonlinear way.

There are two basic hypotheses about the origin of delayed luminescence.

The first one [13] considers the luminescence in photosynthetic material as the visible sign of a minor imperfection in the primary photochemical charge separation, generated by charge recombination. The decay can be connected both to a biequimolecular reaction and to the existence of a continuum of kinetic states with decay constants exponentially distributed; the latter explanation is consistent with the large number of charge carriers and reaction pathways occurring in photosynthesis [1].

The second one asserts that the coherence (coherent states and fields) plays an important role in the functioning of living matter (see, e.g., [14]), and, in particular, might be responsible for the DL spectra of biological systems [15]. According to this hypothesis, in fact, the DL in biological systems originates from a fully coherent field, which is essential for the promotion and control of living processes.

Up to now neither of the two hypotheses has been able to explain the main characteristic of DL. Both models, in fact, predict the hyperbolic law Eq. (1) with α equal to 1 or 2, while according to experimental data, the value of α, which fits the data, varies for various systems and conditions in a large interval (from 1 to 5). Besides this, they are not concerned with the other two properties (b) and (c) of DL.

Recent results of experimentally observed correlation between the DL and chloroplast organization [16] and analogies in certain features of DL spectra from biological and some solid-state systems [17] indicate that this phenomenon in biological systems can be connected with the collective electron states. On the other hand, in view of the long duration of DL and high physiological temperatures of biosystems, it can hardly be connected with delocalized states, such as conventional band electrons or excitons. Based on this, another model to explain the main properties of the DL of simple biological systems has been suggested in [18]. It takes into account that during the charge and energy transfer processes the nonlinear coherent self-trapped electron states

*Email address: brizhik@bitp.kiev.ua
†Email address: demone@dmfci.unict.it

are formed in low-dimensional macromolecular structures. In particular, the model assumes that the DL is connected with the formation and dissociation of localized exciton and electron states (solitons and electrosolitons) which are much more stable than the corresponding delocalized states, and can be created by the preillumination of the sample. This model has been shown to be consistent with the main features of the DL in bio-systems. It also gives a qualitative explanation and reasonably good quantitative fit of the experimental results for the unicellular alga *Acetabularia acetabulum (A.a.)* [18]. In the meantime, as it has been indicated in [18], despite the good χ^2 value achieved in a short time interval, at longer times the precision of the fit decreases and the deviation of the theoretical and experimental time trends of the DL from *A.a*. increases. This can be due to neglecting correlation between solitons in the model. As it will be shown below, the account of soliton correlation results in more linear time trends of DL intensities in a log-log scale at relatively high levels of excitation and kinetics rates. This gives higher precision of the theoretical fit of experimental data for *A.a.* as compared with our previous model.

II. THE MODEL

As it was mentioned in Sec. I, the long duration of DL and its main properties in bio-systems indicate this phenomenon can be connected with coherent electron states in macromolecules. In a biological cell there is a large variety of low-dimensional macromolecules as, for instance, alpha-helical polypeptide proteins, actin filaments, etc., whose structure is represented by the arrays of parallel quasi-one-dimensional (quasi-1D) polypeptide chains formed by the periodically placed peptide groups. The chains are characterized by the strong exchange and/or resonance interaction between the neighboring molecules, while the interaction between the chains is much weaker. From the point of view of electronic structure, these macromolecules are semiconductor-like quasi-1D systems with the filled valence band and empty conduction band, separated by the gap of finite width [19].

These characteristic properties of biological macromolecules favor the existence of coherent collective electron and exciton states, in general, and solitons in particular. The concept of molecular solitons or 1D polaron-type states, which participate in charge and energy transport during the metabolic processes, was first suggested by Davydov and Kislukha [20]. It has been useful to explain numerous phenomena in biological systems [21,22] and some experimental evidence for soliton existence in biological systems has been found [23].

Here we consider the charge transfer processes in systems, which produce photosynthesis. Photosynthesis takes place in chloroplasts, which include so called photosystem I (PSI), that produces nicotinamide adrenine dinucleotide phosphate (NADPH) and has 730 nm maximum in the fluorescence spectrum, and photosystem II (PSII) that participates in the transport of electrons and produces molecular oxygen and has 680 nm maximum (see, e.g., [1,24]). The initial step of photosynthesis is the photon absorption by a pigment system. The captured energy of the photon rapidly migrates to a specific protein complex (reaction center) where it initiates electron transfer chemistry. Rapid charge separation ($\sim$5 ps) occurs and a radical pair state P^F is formed (lifetime $\sim$10 ns). Effective charge separation is increased by the secondary and tertiary chemical reactions (electron transport chain) in PSI and PSII which work in series of the overall scheme

$$H_2O \rightarrow ZP_{680}Q_AQ_B[PQ_{pool}] \rightarrow PC\ P_{700}X \rightarrow NADP^+.$$

Here Z is the electron donor of the PSII reaction center, Q_A and Q_B are the primary and secondary quinone acceptors of PSII, respectively, X is the primary electron acceptor of PSI, the pool of plastoquinone molecules PQ and the plastocyanin PC represent the first and the last component, respectively, of the charge transfer system that connects the two photosystems, $NADP^+$ is the oxidized form of nicotinamide adenine dinucleotide phosphate. The pigments P_{680} and P_{700} are special chlorophyll α molecules, which act as primary electron donors of photosynthetic reaction centers of PSII and PSI, respectively. The complexes $PCP_{700}X$ and $ZP_{680}Q_AQ_B$ are PSI and PSII reaction centers, respectively. Besides the group of the reaction center, PSII includes the light harvesting complex and the complex that releases molecular oxygen.

A. Self-trapped electron states in macromolecules

As it was mentioned above, the PS II photosystem participates in the transport of electrons, and includes transmembrane polypeptide chains with molecular mass greater than 600 kD.

Just in these macromolecules, as well as in micrototubules and actin filaments in alpha-conformation, extra electrons can form electrosolitons [20,21]. When in the electron transfer chain an extra electron is transferred from a donor molecule to one of the subunits of the macromolecule, it affects the nearest surrounding due to the exchange interaction with the nearest neighbors and electron-phonon interaction with hydrogen bonds along a chain. This results in the creation of the local distortion of the chain which, in its turn, plays the role of the potential well for the electron itself and leads to the self-trapping (autolocalization) of an electron. The dynamics of extra electrons in the self-consistent deformation field is described by the system of nonlinear coupled equations, which in the traveling wave approximation in the continuum limit can be reduced to the nonlinear Schrödinger equation [21]

$$i\hbar \frac{\partial \Psi}{\partial t} + J \frac{\partial^2 \Psi}{\partial x^2} + 2JG|\Psi|^2\Psi = E_0\Psi, \tag{2}$$

with the nonlinearity parameter G, determined in the general case by the dimensionless electron-phonon coupling constant g,

$$g = \frac{g_0}{(1-s^2)}, \quad g_0 = \frac{\sigma^2}{2Jw}, \quad s^2 = \frac{V^2}{V_{ac}^2}, \tag{3}$$

and the spectral parameter E_0,

$$E_0 = J\int_0^L \left[\left(\frac{\partial \Psi}{\partial x} \right)^2 - 2G|\Psi|^4 \right] dx. \tag{4}$$

Here $\Psi(x,t)$ is the amplitude of the electron probability distribution, J is the exchange interaction with the nearest neighbors, σ is the constant of electron-phonon interaction, w is the elasticity coefficient of the chain, $w=MV_{\rm ac}^2/a^2$, $V_{\rm ac}$ is the sound velocity in the chain, M is the mass of a unit cell and a is the equilibrium distance between periodically placed monomers in the chain of the length La.

The self-consistent deformation of a chain, $\rho(x,t)$, caused by the electron-phonon coupling, is proportional to the electron probability

$$\rho(x,t)=\frac{\chi}{w}|\Psi(x,t)|^2, \tag{5}$$

and has the energy W

$$W=\frac{MV_{ac}^2}{2a^2}\int_0^L \rho^2 dx. \tag{6}$$

Therefore, the total energy of the excitation, which satisfies Eq. (2) and is bound with the deformation field, also includes the energy of deformation

$$E=E_0+W. \tag{7}$$

In particular, in the case of one extra electron the nonlinearity parameter equals the electron-phonon coupling constant: $G=g$. An exact analytical solution of Eq. (2) is given by the function

$$\Psi_s(x,t)=\frac{1}{2}\sqrt{g}\,\frac{\exp[i(qx-\Phi_s(t))]}{\cosh[g(x-Vt/a)/2]}, \tag{8}$$

which describes the self-trapped state called the soliton, which moves together with the local distortion with a certain velocity $V<V_{\rm ac}$ to the opposite end of the macromolecule. Here and in what follows functions $\Phi_i(t)$ are the phases of corresponding solutions, and q is the wave number, which is connected with the velocity by the relation $q=\hbar V/(2Ja)$.

Substituting Eq. (8) into Eqs. (4) and (7), we determine that the total energy of a soliton state is lower than the energy of the lowest delocalized state, which coincides with the energy of the conduction band bottom, by the value E_s [9,10]

$$E_s(0)=-\frac{1}{12}Jg_0^2. \tag{9}$$

In the case when there are two extra electrons with opposite spins, they form a singlet bisoliton [25,26], which describes a bound state of two electrons localized within the same potential well created by the distortion of a chain. In this case the nonlinearity parameter in Eq. (2) reads as $G=2g$. The bisoliton wave function is

$$\Psi_{\rm bs}(x,t)=\sqrt{\frac{g}{2}}\frac{\exp[i(qx-\Phi_{\rm bs}(t))]}{\cosh[g(x-Vt/a)]}. \tag{10}$$

According to Eqs. (4)–(7), the energy of a bisoliton at rest is

$$E_{\rm bs}(0)=-\tfrac{2}{3}Jg_0^2. \tag{11}$$

If the number of extra electrons in a chain is essentially bigger than one, the theoretical model predicts the existence of coherent many-electron states [27,28]. At small values of electron concentration such a state is described by Eq. (2), in which $G=2g$, and the wave function satisfies the periodic condition $\Psi(x+l,t)=\Psi(x,t)$. It accounts for the fact that in the average per each period l, there are two electrons with opposite spins which, in the limit of a very large period, can be approximated by the bisoliton function Eq. (10) [26,27]. The period of function l and concentration of bisolitons δ are connected by a relation $l=1/\delta$. A periodical solution of Eq. (2) is given by a cnoidal wave, the envelope of which is described by a periodic Jacoby function

$$\Psi_{\rm cn}(x,t)=\sqrt{\frac{g}{2}}E^{-1}(k)dn\left(\frac{g(x-Vt/a)}{E(k)},k\right)\times\exp[i(qx-\Phi_{\rm cn}(t))]. \tag{12}$$

Here $E(k)$ is a complete elliptic integral of the second kind, the modulus of which k is determined by the space period of the function, and, hence, by bisoliton concentration $\delta=1/l$, according to the following relation:

$$gl=2E(k)K(k), \tag{13}$$

with $K(k)$ being a complete elliptic integral of the first kind. The energy of the cnoidal wave per period, i.e., the energy per bisoliton in a coherent superlattice, reads as

$$E_{\rm cn}(0)=2J\int_0^l\left[\left(\frac{\partial\Psi}{\partial x}\right)^2-2g_0|\Psi|^4\right]dx. \tag{14}$$

Substituting the explicit expression of the wave function Eq. (12) into Eq. (14) and carrying out the integration, we find that the energy Eq. (7) of such cnoidal wave is function of the concentration of bisolitons

$$E_{\rm cn}(0)=-\tfrac{2}{3}Jg_0^2[E(k)(2-k^2)+K(k)(1-k^2)]E^{-3}(k). \tag{15}$$

The analysis of expression (13) shows that the inequality takes place at $l>l_{\rm cr}=\pi^2/2g_0$. This means, there is some critical value of bisoliton concentration

$$\delta_{\rm cr}=\frac{2g_0}{\pi^2}, \tag{16}$$

above which, at $\delta>\delta_{\rm cr}$, the cnoidal wave does not exist because of the too strong repulsion between the electrons. It also follows from Eq. (15) that the energy gap that separates the localized electron level from the delocalized states in the conduction band vanishes when δ tends to $\delta_{\rm cr}$.

B. Kinetics of the delayed luminescence

We assume the following general scheme of the process of delayed luminescence. Electrons released in the ionized centers of luminescence (the charge separation complexes), with a certain probability are self trapped in the macromol-

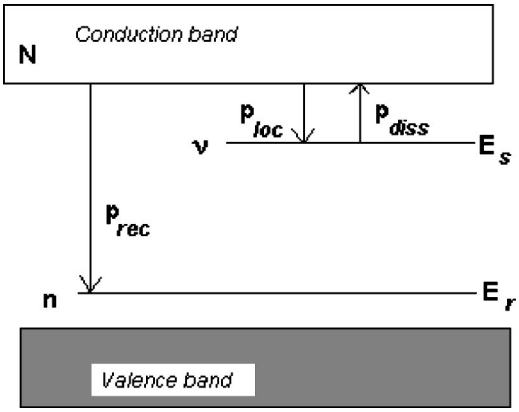

FIG. 1. The energy level scheme of the DL in the presence of the self-trapped states. Here E_r is the energy level of the reaction center, and E_s is the level of a self-trapped state; n is the number of ionized reaction centers, N is the number of free electrons in the conduction band, and ν is the number of electrons in localized (bi)soliton states; $p_{\rm diss}$ is the rate of (bi)soliton dissociation, $p_{\rm rec}$ is the rate of electron-hole recombination at the reaction center, and $p_{\rm loc}$ is the rate of electron localization.

ecules. The luminescence arises from the decay of these localized states into the conductive electron band with the following fast transition into the recombination centers, i.e., ionized centers of luminescence. A comparison of the experimentally measured fluorescence and DL emission spectra [16] reveals no energy shift, therefore, we neglect the probability of the direct transitions of electrons from the self-trapped states into reaction centers. The spatial arguments support this model as well: a soliton is localized within a few lattice sites in a macromolecule and can transit to the distant reaction center via the conducting band by back reaction. The energy level diagram of this process is shown in Fig. 1. According to the above, the electron-hole recombination processes determine the intensity of DL

$$I=-\frac{dn}{dt}, \tag{17}$$

where n, the number of the ionized reaction centers, is connected with the number of free electrons in the conduction band N and the number of electrons in localized (bi)soliton states ν by the relation

$$n=N+\nu. \tag{18}$$

In a biological system (cells, organisms, etc.) there is a large number of macromolecules, therefore the mean-field description is applicable and the following system of equations is valid:

$$\frac{dn}{dt}=-p_{\rm rec}Nn, \tag{19}$$

$$\frac{dN}{dt}=p_{\rm diss}\nu-p_{\rm rec}Nn-p_{\rm loc}N(\nu_0-\nu), \tag{20}$$

$$\frac{d\nu}{dt}=-p_{\rm diss}\nu+p_{\rm loc}N(\nu_0-\nu). \tag{21}$$

Here ν_0 is the number of available localized states, determined by the maximum available concentration of (bi)solitons in a macromolecule: $\nu_0=2\delta_{\rm cr}$, where $\delta_{\rm cr}$ is given by Eq. (16); $p_{\rm diss}$ is the rate of (bi)solitons dissociation [29–31], $p_{\rm rec}$ is the rate of electron-hole recombination at the reaction center, and $p_{\rm loc}$ is the rate of electron localization which is determined by the energy of localization in the corresponding state

$$p_{\rm loc}=\frac{E_{\rm loc}}{\hbar}. \tag{22}$$

All rates are calculated per unit time.

In the case when solitons are noncorrelated (at very small concentrations, in not long enough macromolecules, etc.), electrons localize in the independent (bi)soliton states, and the probability of electron localization, according to Eqs. (9) or (11), does not depend on soliton concentration (this corresponds to the model suggested in [18]). In the opposite case of strongly correlated coherent electrons the dependence of the energy of the localized level on the concentration of electrons is essential. In this latter case, which is the aim of the present study, the energy of electron localization is

$$E_{\rm loc}=\tfrac{1}{2}[E_{\rm del}(0)-E_{\rm cn}(0)]=\tfrac{1}{3}Jg_0^2F(k), \tag{23}$$

where $E_{\rm del}(0)$ is the electron energy in a delocalized state, $E_{\rm cn}(0)$ is determined in Eq. (15),

$$F(k)=\frac{(1+k_1^2)E(k)K(k)+k_1^2K^2(k)-3E^2(k)}{E^3(k)K(k)}, \tag{24}$$

and k_1^2 is additional elliptic modulus: $k_1^2=1-k^2$. At the concentrations of bisolitons lower than the critical value Eq. (16), the relation $k_1^2\ll 1$ is fulfilled. In this case the complete elliptic integrals take the asymptotic values [32]

$$E(k)\approx 1, \quad K(k)\approx\log\frac{4}{k_1}, \quad k_1^2\ll 1, \tag{25}$$

and from Eq. (13) we get the explicit relation between the additional modulus and bisoliton concentration:

$$k_1^2\approx 16\exp\left(-\frac{g_0}{\delta}\right). \tag{26}$$

In the same limit $k_1^2\ll 1$ we find from Eqs. (24)–(25)

$$F(k)\approx\left(1+k_1^2-k_1^2\log\frac{4}{k_1}-\frac{3}{\log\dfrac{4}{k_1}}\right)\approx\left(1-\frac{\delta}{\delta_0}\right), \tag{27}$$

where $\delta_0=g_0/6$. Therefore, the probability of electron localization takes the value

$$p_{\mathrm{loc}}=p_0\left(1-\frac{\nu}{\nu_0}\right), \tag{28}$$

where

$$p_0=\frac{Jg_0^2}{3\hbar}, \quad \nu=2\delta, \quad \nu_0=2\delta_0. \tag{29}$$

The rate of (bi)soliton dissociation p_{diss} is much smaller than the decay rate of band electrons [29]. Hence, the relation $N \ll \nu$ is fulfilled, which corresponds to the quasistationary regime,

$$\frac{dN}{dt} \ll \frac{d\nu}{dt}. \tag{30}$$

From Eqs. (19)–(21) and (28) in the approximation Eq. (30) we get

$$N(t) \approx \frac{p_{\mathrm{diss}}\nu(t)}{p_{\mathrm{rec}}n(t)+p_0(\nu_0-\nu(t))\left[1-\dfrac{\nu(t)}{\nu_0}\right]}. \tag{31}$$

This together with the relation Eq. (17) determines the time dependence of the number of ionized reaction centers

$$\frac{dn}{dt} \approx -\frac{p_{\mathrm{diss}}n^2}{\gamma\nu_0+n(1-2\gamma)+\gamma n^2/\nu_0}, \tag{32}$$

where the notation is introduced

$$\gamma=\frac{p_0}{p_{\mathrm{rec}}}. \tag{33}$$

Integrating Eq. (32) with the initial condition $n(t=0)=n_0$, the following relation can be obtained:

$$p_{\mathrm{diss}}t=(1-\gamma)\log\frac{n_0}{n}+\gamma\nu_0\left(\frac{1}{n}-\frac{1}{n_0}\right)-\frac{\gamma}{\nu_0}(n-n_0). \tag{34}$$

Equations (17), (32)–(34) determine the intensity and kinetics of the delayed luminescence. It is convenient to introduce the dimensionless variables

$$\tau=p_{\mathrm{diss}}t, \quad y=\frac{n}{n_0}, \quad x_0=\frac{n_0}{\nu_0}, \quad I(\tau)=\frac{\mathrm{I}(t)}{p_{\mathrm{diss}}\nu_0}, \tag{35}$$

in which the system of equations for the intensity of DL takes the suitable for numerical study form of:

$$I(\tau)=\frac{x_0^2y^2}{x_0y+\gamma(1-x_0y)^2}, \tag{36}$$

$$\tau=(2\gamma-1)\log(y)+\frac{\gamma}{x_0}\left(\frac{1}{y}-1\right)-\gamma x_0(y-1). \tag{37}$$

Recall the DL within the noncorrelated model [18] is described by the system of equations

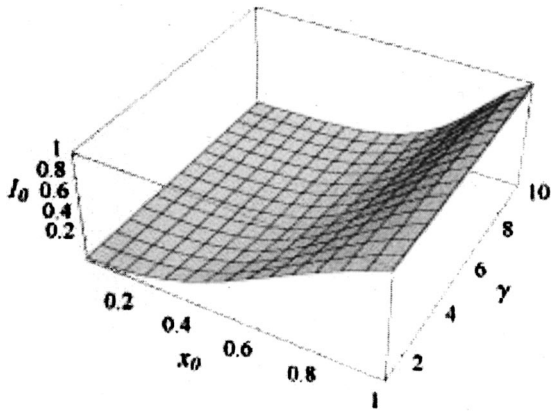

FIG. 2. Theoretical dependence of the initial value of the DL on the level of excitation x_0 and the kinetics rate γ within the correlated model, as given by Eqs. (36)–(37).

$$I_{\mathrm{nc}}(\tau)=\frac{x_0^2y^2}{x_0y+\gamma(1-x_0y)}, \tag{38}$$

$$\tau=(\gamma-1)\log(y)+\frac{\gamma}{x_0}\left(\frac{1}{y}-1\right) \tag{39}$$

that formally coincide with the equations, obtained in [33] for crystallophosphors, and which are valid in a more general case for systems possessing the band structure with the collectivised electron/exciton states.

Analysis of Eqs. (36) and (37) shows that the kinetics of the DL, as in our previous model [18], depends on the two basic parameters: (i) on the kinetics rate γ, determined by Eq. (33) as the ratio of the characteristic rates of the localization and recombination processes, and (ii) on the level of excitation, $x_0=n_0/\nu_0$.

According to Eqs. (36) and (37), the initial intensity $I_0=I(\tau=0)$ in the general case is a nonlinear function of the level of excitation x_0:

$$I_0=\frac{x_0^2}{x_0+\gamma(1-x_0)^2}, \tag{40}$$

which becomes linear in the limit of zero values of γ, only. The dependence of the initial intensity on the level of excitation x_0 for various kinetics rates $\gamma \ll 1$ is shown in Fig. 2. Indeed, the experimental study of the DL of the biological systems reveals the nonlinear dependence of I_0 on the intensity of the stimulating light [11]. For a comparison, this dependence within the noncorrelated model Eqs. (38) and (39) is shown in Fig. 3. At small values of the kinetics rates $\gamma \ll 1$ (not shown in the figures) both models predict similar behavior of $I_0(x_0)$. Increasing the value of γ, the deviation between the two models increases and is significant even at $\gamma<1$. The bigger the value of γ, the bigger the difference between the correlated and noncorrelated models. This dependence within the former model at $\gamma \gg 1$ is given by a nonlinear curve with the saturation, while it can be approximated by a linear dependence in a wide interval of $0 \leqslant x_0 < x_{\mathrm{cr}} < 1$ within the latter model (compare Figs. 2 and 3).

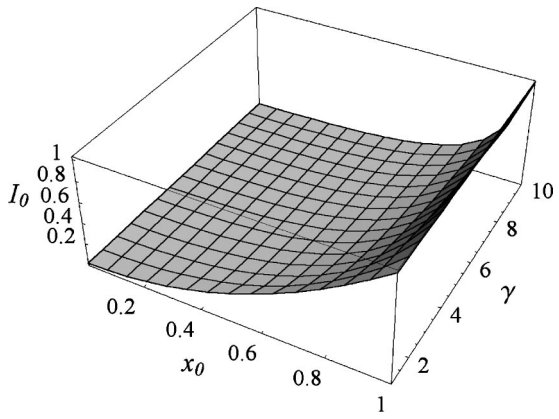

FIG. 3. Theoretical dependence of the initial value of the DL on the level of excitation x_0 and the kinetics rate γ, within the noncorrelated model, as given by Eqs. (38) and (39).

The difference between the two models is also revealed by a comparison of the time trends of the intensity of DL in large time intervals (see below).

It is worth noting that while for most of the conventional solid-state systems the excitation level practically always reaches saturation, i.e., $x_0=1$, the stimulating light used in our study of biological systems is of low intensity, therefore, in this latter case the most probable is the regime $x_0<1$. For the sake of clarity the dependence of the DL decay according to Eqs. (36) and (37) on the excitation level x_0 is shown in Fig. 4.

As in our previous model [18], different components of the emission spectrum correspond to electron transitions from different energy levels of electrons in the conduction band. Hence, in the first approximation every component should obey Eqs. (36) and (37) with the same value of γ, and therefore, the time trends of various components of the emission spectrum should be identical. Indeed such behavior has been observed experimentally in [16] for the emission spectra of *A.a.* samples.

III. COMPARISON WITH EXPERIMENTAL DATA

We have applied our theoretical model to explain some of the experimental data on the DL of unicellular alga *A.a*,

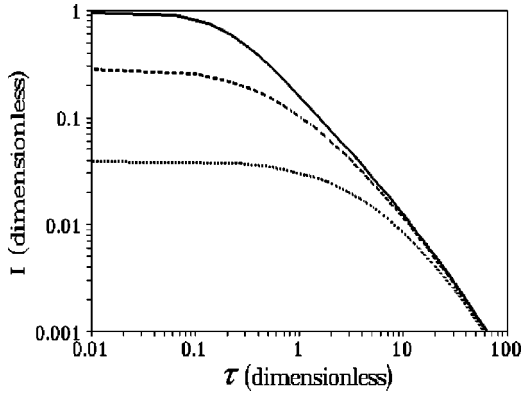

FIG. 4. Theoretical dependence of the DL decay on the excitation level x_0 according to Eqs. (36)–(37). Curves are calculated at the kinetic rate $\gamma=10$, and different values for x_0: $x_0=1$ (solid line), $x_0=0.7$ (dashed line), and $x_0=0.4$ (dotted line), respectively.

TABLE I. Range of variability of the excitation level x_0 at the different intensities of the stimulating light I_{st}.

I_{st}	x_0
100%	0.76–0.85
70%	0.66–0.77
50%	0.59–0.69
20%	0.35–0.45
10%	0.22–0.29

which seems to be a system admitting the existence of correlated self-trapped electron states. In particular, in *A.a* there are very long macromolecules, like actin filaments and microtubules, which form the cytoskeleton of cells [34–36] and are responsible for the motility of organelles and the streaming of cytoplasma in the whole. These microfilaments have largely variable length from 10–20 to a few hundreds of subunits; they have a double-chain helical structure [37], and in the presence of the fimbrin protein they are bundled together into parallel arrays. These macromolecules are good candidates for a system in which a large number of correlated electrosolitons can be excited under certain conditions.

Experiments consisted of illuminating the sample, consisting of an *A.a.* cell placed in a plastic Petri dish filled with artificial sea water, with a short light pulse (less than 3 ms) of selected wavelength and measuring the time dependence of the number of photons emitted. In the results reported below we used stimulating light of 450 nm at the maximum intensity $I_{max}=2.4\times10^{16}$ photons/cm^2/s. The illumination was obtained filtering a flash lamp (Metz 45CL1) with a broadband filter (40 nm full width half maixmum, Andover 110FA40). Starting from this maximum value of illumination intensity, reduced intensities I_{st} of the stimulating light were obtained by using metallic neutral density filter (Andover No. FN46). In particular, we used as stimulating light I_{st} the values 100%, 70%, 50%, 20%, 10% of the maximum intensity I_{max}. The experimental setup, materials, and method are described elsewhere [10,12,16].

To apply the model to experimental data, it is necessary to estimate the numerical value of γ. Using the parameter values for polypeptides [22] we get from Eq. (29) that $p_0\approx10^{11}$ s^{-1}. The characteristic rate of charge recombination p_{rec} varies in the interval from 10^9 to 10^{11} s^{-1} [1]. Substituting these values in the definition Eq. (33), we get $\gamma=1-100$.

According to our experimental data, the total number of photons emitted depends on the intensity of the impinging photons in a nonmonotonous way [38], reaching some saturation value. In the current experiments with algae the maximum intensity of the stimulating light 100%, i.e., $I_{st}=I_{max}$, was lower than the saturation value shown in Fig. 4 [38], which corresponds to the excitation level $x_0=1$. So, using the data of Fig. 4, Ref. [38] and starting with some value of the impinging photons corresponding to saturation, the values of the excitation level x_0 for the intensities used have been estimated. Next, from the relation between the values of I_0 and x_0 for any two intensities of impinging light the estimate of γ has been obtained, using relation (38). In order to

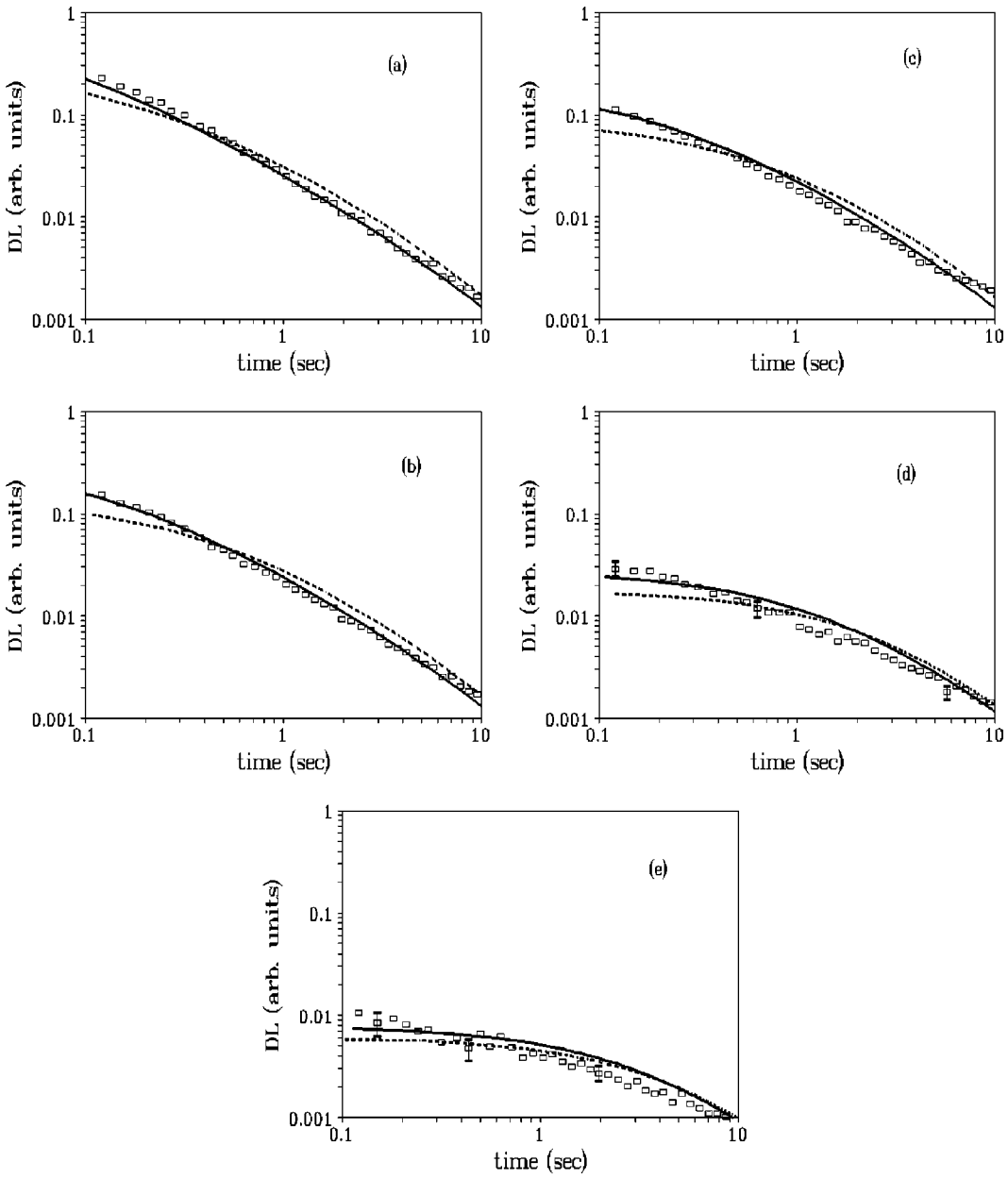

FIG. 5. Time trends of the intensities of DL from *A.a.* at different intensities of the stimulating light I_{st}. Symbols show normalized experimental data, solid and dashed lines correspond to theoretical fit within the coherent correlated and noncorrelated models, respectively, at $\gamma=10$, for the following values of I_{st} and x_0: (a) $I_{st}=I_{max}$, $x_0=0.85$; (b) $I_{st}=0.70\ I_{max}$, $x_0=0.71$; (c) $I_{st}=0.50\ I_{max}$, $x_0=0.62$; (d) $I_{st}=0.20\ I_{max}$, $x_0=0.35$; (e) $I_{st}=0.10\ I_{max}$, $x_0=0.22$. In the figures where the error bars are not reported, the errors are as large as the size of the marker.

take into account all causes of error we considered an uncertainty of 20% on the starting point of the evaluation procedure. From this analysis determined that the maximum intensity of the stimulating light, $I_{st}=I_{max}$, corresponds to x_0 values in the interval $0.76\leqslant x_0\leqslant 0.85$ and correspondingly γ should vary in the interval $6<\gamma<12$. Table I reports the range of variability of the x_0 values at the reduced intensities used in the experiment.

Our calculations for the DL kinetics for *A.a.* at a stimulating light of 450 nm show that a reasonably best fit (reduced χ^2 values ranging from 1.6 to 3.8) of the experimental data at the five different intensities of the impinging light in the whole time interval of measurements is obtained at $\gamma=10$, with $p_{diss}=5.2\ s^{-1}$. These results are represented in Fig. 5: symbols show the experimental data normalized to the highest value of the initial intensity, and solid and dashed lines correspond to the fit within the correlated and noncorrelated [18] theoretical models, respectively.

IV. CONCLUSION

Both mechanisms of the DL, suggested in [18] and in the present paper, are based on the assumption that the photoinduced light emission of biological systems is connected with

the self-trapped electron states that provide the charge and energy transfer processes. In particular, in green plants such an emission is connected with the processes occurring in chloroplasts, and is related to the presence of self-trapped soliton levels in macromolecules forming the photosystem and the cytoskeleton of a cell. Accordingly, a correlation between the DL and chloroplast organization has been experimentally observed in *A.a*. [16]. The preliminary results of the application of our model to the DL from bio-systems that do not possess photosystems, in particular, from yeast, also show satisfactorily good agreement (this work is in progress).

Worth noting, the two mechanisms of the DL, discussed here, can complement each other. Realization of one or another depends on the biological system and the corresponding conditions. Both mechanisms assume the DL is connected with the presence of self-trapped electron states in macromolecules, where one model accounts for the noncorrelated soliton states, and the present one accounts for the correlated ones. One of the reasons of the correlated behavior, like in unicellular alga *A.a.*, and less important or negligibly small in other systems with shorter macromolecules. Another reason can be due to the state of the metabolic activity of a system that determines the number of (bi)solitons and the level of their coherence.

The above analysis shows that the nonlinear coherent model of the DL provides a qualitative and quantitative explanation of the main characteristic features of the DL spectra from *A.a*. These include the kinetics of time decay, the nonlinear dependence on the intensity of the stimulating light, and the same time trend for all the emission spectral components. In addition, the correlated model gives higher precision of the theoretical fit of experimental data for *A.a*. in the wide interval of intensities of the stimulating light and in the whole time interval of experimental measurements, as compared with the noncorrelated model. The correlation between the DL and the state of the organism is easily explained within this model. The change of the physiological conditions affects the processes of charge transfer in the whole, and electrosoliton transfer in particular, which is reflected in the change of the parameter γ, and hence, in the change of the time trend of DL. When the changes in the organism are reversible, the changes of the DL spectra are reversible and *vice versa* at the irreversible change the spectrum is not recovered [10,12].

ACKNOWLEDGMENT

One of us, L.B., acknowledges financial support from INFM, Italy for a stay in Catania.

[1] P. A. Jursinic, in *Light Emission by Plants and Bacteria*, edited by J. Amesz, Govindjee, and D. C. Fork (Academic, London, 1986), p. 291.
[2] J. Slawinski and D. Slawinska, in *Chemistry and Bioluminescence*, edited by J. G. Barr (Marcell Dekker, New York, 1985), p. 495.
[3] T. V. Veselova, V. A. Veselovsky, A. B. Rubin, and V. Z. Bocharov, Physiol. Plant. **65**, 493 (1985).
[4] B. Chwirot and F. A. Popp, Folia Histochemica Cytobiologica **29**, 155 (1991).
[5] M. W. Ho, X. Xu, S. Ross, and P. T. Saunders, in *Recent Advances in Biophoton Research*, edited by F. A. Popp, K. H. Li, and Q. Gu Q. (World Scientific, Singapore, 1992), p. 287.
[6] R. Neurohr, in *Recent Advances in Biophoton Research*, edited by F. A. Popp, K. H. Li, and Q. Gu (World Scientific, Singapore, 1992), p. 375.
[7] F. Grasso, C. Grillo, F. Musumeci, A. Triglia, G. Rodolico, F. Cammisuli, C. Rinzivillo, G. Fragati, A. Santuccio, and M. Rodolico, Experientia **48**, 10 (1992).
[8] R. Van Wijk, H. Van Aken, W. P. Mei, and F. A. Popp, J. Photochem. Photobiol., B **18**, 75 (1993).
[9] F. Musumeci, A. Triglia, F. Grasso, A. Scordino, and D. Sitko, Nuovo Cimento D **16**, 65 (1994).
[10] A. Scordino, A. Triglia, F. Musumeci, F. Grasso, and Z. Rajfur, J. Photochem. Photobiol., B **32**, 11 (1996).
[11] F. Musumeci, A. Scordino, and A. Triglia, Riv. di Biologia/ Biology Forum **90**, 95 (1997).
[12] M. W. Ho, F. Musumeci, A. Scordino, and A. Triglia, J. Photochem. Photobiol., B **45**, 60 (1998).
[13] J. Lavorel, J. Breton, and M. Lutz, in *Light Emission by Plants and Bacteria*, edited by J. Amesz, Govindjee, and D.C. Fork (Academic, London, 1986), p. 57.
[14] F.A.Popp, in *Electromagnetic Bio-Information*, edited by F.A. Popp, U. Warnke, H. L. König, and W. Peschka (Urban and Schwarzenberg, München, 1989), p. 193.
[15] F. A. Popp and K. H. Li, Int. J. Theor. Phys. **32**, 1573 (1993).
[16] R. Van Wijk, A. Scordino, A. Triglia, and F. Musumeci, J. Photochem. Photobiol., B **49**, 142 (1999).
[17] A. Scordino, A. Triglia, and F. Musumeci, J. Photochem. Photobiol., B **56**, 181 (2000).
[18] L. Brizhik, A. Scordino, F. Musumeci, and A. Triglia, Europhys. Lett. **52**, 238 (2000).
[19] I. I. Ukrainskii and S. L. Mironov, Teor. Eksp. Khim. **15**, 144 (1979) (in Russian).
[20] A. S. Davydov and N. I. Kislukha, Phys. Status Solidi B **59**, 465 (1973).
[21] A. S. Davydov, *Solitons in Molecular Systems* (Reidel, Dordrecht, 1985).
[22] A. C. Scott, Phys. Rep. **217**, 1 (1992).
[23] G. Careri, U. Buontempo, F. Galluzzi, A. C. Scott, E. Gratton, and E. Shyamsunder, Phys. Rev. B **30**, 4689 (1984).
[24] L. Stryer, *Biochemistry*, 3rd ed. (W.H. Freeman, New York, 1988).
[25] L. Brizhik and A. Davydov, J. Low Temp. Phys. **10**(7), 748 (1984).
[26] L.S. Brizhik, J. Biol. Phys. **19**, 123 (1993).
[27] L. Brizhik and A. Davydov, J. Low Temp. Phys. **10**(4), 358 (1984).
[28] A.A. Eremko, Phys. Rev. B **46**, 3721 (1992).
[29] A. A. Eremko, in *Davydov's Soliton Revisited*, edited by P. L.

Christiansen and A. C. Scott (Plenum, New York, 1990), p. 429.
[30] L. Brizhik, L. Cruzeiro-Hansson, and A. Eremko, J. Biol. Phys. **24**, 19 (1998).
[31] A. S. Davydov and A. A. Eremko, Ukr. Fiz. Zh. **22**, 881 (1977).
[32] *Handbook of Mathematical Functions*, edited by M. Abramowitz and I.A. Stegun, National Bureau of Standards, Applied Mathematics Series, Vol. 55 (NBS, Washington, DC, 1964).
[33] E. I. Adirovitch, *Some Problems of the Theory of Luminescence of Crystals* (Technical and Theoretical Literature Publication Inc., Moscow-Leningrad, 1951) (in Russian).
[34] N. Kamiya, Bot. Mag. Tokyo **99**, 444 (1986).
[35] H. U. Koop and O. Kiermayer, Protoplasma **102**, 147 (1980).
[36] D. Menzel, Protoplasma **179**, 166 (1994).
[37] S. L. Wolfe, *Molecular and Cellular Biology* (Waldsworth, Belmont, CA, 1993).
[38] A. Scordino, F. Grasso, F. Musumeci, and A. Triglia, Experientia **49**, 701 (1993).